UNIVERSITY OF CALIFORNIA
RIVERSIDE

Hyaluronic Acid Hydrogels Loaded with Curcumin-Coated Magnetic Nanoparticles for Angiogenesis in Bone Tissue Engineering

A Thesis submitted in partial satisfaction
of the requirements for the degree of

Master of Science

in

Bioengineering

by

Radha J. Daya

September 2017

Thesis Committee:
Dr. Huinan Liu, Chairperson
Dr. Xiaoping Hu
Dr. Hyle Park

The Thesis of Radha J. Daya is approved:

_____

_____

_____

Committee Chairperson

University of California, Riverside

ACKNOWLEDGEMENTS

I would like to thank my advisor, Dr. Huinan Liu for giving me the opportunity to join her lab, for her supporting me to complete my MS thesis, and for fostering a diverse lab in which I was able to receive guidance from many different perspectives. I would also like to thank Dr. Hyle Park and Dr. Xiaoping Hu for serving as a part of my committee and providing me with support and feedback to be able to complete my thesis and thesis defense.

My journey would not have been possible without the support of the current and former members of the Biomaterials and Nanomedicine Lab group. Specifically, Naiyin Zhang for getting me started with my project and supporting me for the remainder of my project as a peer and a friend. I would also like to thank my friends, Nhu-Y Nguyen and Cheyann Wetteland, two incredibly dedicated and passionate students who supported me every step of the way. I have always been inspired by your resilience. Both of you welcomed me into the lab, gave me the confidence to develop my project, and provided me with guidance and feedback and encouraged me to continue when I felt like giving up. I learned so much from your insight and experience.

I would like to thank Dr. Hyle Park for providing me with support in making decisions when I was confused about how to make the most out of my graduate school experience. He also offered open ears in times of stress and anxiety and proved to be an excellent graduate advisor and a member of my defense committee.

And finally I would like to thank my sisters and friends who experienced my highs and lows of graduate school and answered all of my questions about science, life,

graduate school, grammar, Photoshop, and how to stay motivated, etc. Thank you for your unconditional support: Krishna Patel, Mira Daya, Kingsley Andersen, Alice Cheng, Courtney Jeung, Jeremy Hurtado, Shereen Aldaimalani, Riddhi Khatri, Sana Hussain, Alex Reardon and many more. I would also like to thank my parents for their unconditional love and support and for coping with me being far away from home for the past 7 years.

Dedication

I dedicate this thesis to
My lifelines:
Krishna Patel
Mira Daya
Kingsley Andersen
Alice Cheng
for their unconditional love and support that has made it possible for me to keep fighting.

ABSTRACT OF THE THESIS

Hyaluronic Acid Hydrogels Loaded with Curcumin-Coated Magnetic Nanoparticles for Angiogenesis in Bone Tissue Engineering

by

Radha J. Daya

Master of Science, Graduate Program in Bioengineering
University of California, Riverside, September 2017
Dr. Huinan Liu, Chairperson

Abstract

Tissue engineering, the combination of cells, scaffolding materials, and biochemical signals, is being extensively researched for tissue generation and regeneration. The potential to generate tissue and organs can combat the limited availability of organ and tissue donors. To guarantee successful tissue engraftment, a sufficient availability of oxygen and nutrients must be provided. This can be done by adding angiogenic properties to therapy [1-4]. The expansion of existing vasculature to the site of repair can increase success rates of transplant and engraftment. Bone marrow stromal cells (BMSCs) can allow bone repair and regeneration and also secrete vascular endothelial growth factor (VEGF), which plays an important role in blood vessel formation and endothelial cell recruitment. Hyaluronic acid hydrogels provide a 3D microenvironment that mimics in vivo conditions and enhances cell viability and function. Iron oxide magnetic iron oxide nanoparticles have been shown to maintain scaffold dexterity while also enhancing cell alignment, viability,

and function. Curcumin is a naturally occurring protein that is being studied for wound healing and angiogenic properties. Curcumin has also been shown to act as a stabilizing surface modifier which prevents the oxidation of iron oxide nanoparticles [13]. When combined, a magnetic hyaluronic acid hydrogel loaded with curcumin and BMSCs can be localized to site of injury by magnetic guidance for bone regeneration and angiogenesis. Curcumin coated iron oxide nanoparticles encapsulated in a hyaluronic acid hydrogel were evaluated in this thesis. The nanoparticles and magnetic hydrogel were synthesized and characterized [25]. Cell adhesion and viability studies were performed with the materials, and post-culture media was evaluated for changes of VEGF release in samples with developed materials and controls. Results suggest that hyaluronic acid hydrogels and curcumin coated iron oxide nanoparticles allowed for enhanced cell adhesion and morphology, and increased the total amount of VEGF production by BMSCs.

Keywords: Magnetic Nanoparticles (MNPs), Iron Oxide (Fe_3O_4), nanoparticles, hyaluronic acid (HyA), Bone Marrow Derived Mesenchymal Stem Cells (BMSCs), Dulbecco's Modified Eagle's Media (DMEM), revised Simulated Body Fluid (rSBF)

Table of Contents

List of Figures

1. Introduction

Tissue engineering is the generation of functional tissue through the culture of stem cells in the presence of scaffolding materials and growth factors or biochemical signals to improve viability and differentiation. Tissue engineering and stem cell transplantation have gained immense attention in the past decade as a potential method to promote functional regeneration of damaged tissues due to their benefits over traditional autograft and allograft procedures. The use of surgical autograft and allograft procedures for bone repair requires invasive surgeries and is limited by donor scarcity and immune rejection. Conversely, tissue engineering involves the development of bioabsorbable scaffolds from synthetic and natural materials, which are non-immunogenic and do not require a donor. Researchers have shown regeneration in several tissue types including bone, liver, kidney, and cardiac tissue [1-6]. Bone tissue requires a scaffolding material to represent a three dimensional, artificial extracellular matrix to maintain cell viability, promote cell attachment and differentiation, and allow for mineralized bone formation [7-10]. However, several challenges still exist when transplanting engineered tissue into the body. One such challenge is providing the new tissue with adequate nutrients and oxygen flow for survivability and the diffusion of waste products. Functional vasculature is an essential component for the viability of any metabolically active tissue. Angiogenesis is the rapid growth of new capillaries and can be enhanced by the presence of many growth factors, one of which is vascular endothelial growth factor (VEGF), which shows promise in enhancing vascularization of engineered tissues. Bone tissue engineering is one field that has benefited from proangiogenic response, based on the need for vascular supply during

healing. Interestingly, studies have shown that bone marrow derived stem cells (BMSCs) can produce VEGF [11, 12].

Magnetic nanoparticles (MNPs) have been extensively researched in the past decade for their application in a number of therapies and techniques: as a contrast agent to enhance magnetic resonance imaging (MRI) for medical diagnostics, as hyperthermia agents for cancer treatment, as drug carriers to improve drug delivery to targeted sites, and for tissue repair [25]. Stabilizing agents can modify the surface of MNPs by co-precipitation and allow for the introduction of additional functionality on the nanoparticle surface [13, 14]. One such stabilizing agent is curcumin (diferuloylmethane)—(1,7-bis(4-hydroxy-3-methoxyphenyl)-1,6-hepadiene-3,5-dione), which is found in turmeric and has been widely studied for its protective biological effects. Previous studies have evaluated curcumin as an anti-angiogenic agent for cancer treatments. However, in non-cancerous wounds, curcumin has been shown to enhance neovascularization and this study aims to take advantage of this effect for angiogenesis of bone constructs to provide sufficient oxygen and nutrient flow to the site of bone repair. Use of curcumin as a surfactant for magnetic iron oxide nanoparticles may allow for controlled release of curcumin and protection of magnetic iron oxide from oxidation to its less magnetic form [13]. Curcumin has previously been shown to enhance secretion of VEGF in endothelial progenitor cells, which plays an important role in the formation of blood vessels [15-17]. As a result, curcumin-coated MNPs are a promising material for controlled enhancement of angiogenesis.

Polymer scaffolds are used in tissue engineering as delivery vehicles for bioactive molecules, space fillers, and as three-dimension molds to organize cells to enhance the formation of a target tissue. Synthetic degradable hydrogels have emerged as an effective way to deliver cells through injection and maintain those cells in a desired area [2, 6]. Hydrogels synthesized using hyaluronic acid (HyA) are appealing scaffold materials due to their structural similarity to the extracellular matrices of many tissues. Hyaluronic acid is a protein found in the extracellular matrix of soft tissue and is therefore non-immunogenic and biocompatible [12]. Hyaluronic acid hydrogels were utilized as a matrix for curcumin-coated MNPs due to their biocompatibility and history as a well-established injectable material for tissue applications.

The objective of this study was to evaluate the effect of bare and hydrogel-loaded curcumin and curcumin-coated MNPs on BMSC activity, with emphasis on VEGF secretion. Curcumin coated magnetic iron oxide nanoparticles (CMNPs) were synthesized from a previously published co-precipitation method. Morphology, size, ferromagnetic response, cytocompatibility, and effect on VEGF secretion was evaluated for CMNPs. The HyA loaded with CMNPs showed potential for proangiogenic bone tissue engineering applications.

2. Materials and Methods

2.1 Properties of Curcumin Coated Iron Oxide Nanoparticles

2.1.1 Synthesis of Curcumin Coated Iron Oxide Nanoparticles

Curcumin coated iron oxide (Fe_3O_4) nanoparticles were synthesized and coated using a previously described co-precipitation method [13]. Briefly, $FeCl_3$ (#169430010, Sigma-Aldrich, St. Louis, MO) and $FeCl_2 \cdot 4H_2O$ (#44939, Sigma-Aldrich, St. Louis, MO) powder with a molar ratio of 2:1 were dissolved in 10mL deionized water (DI water; Milli-Q Integral Water Purification System, EMD Millipore, Billerica, MA) and then added to 40mL of deionized water, in a three-neck round bottom flask under a constant flow of nitrogen gas, and heated to 40 ºC. A solution of 10 wt% curcumin in dimethylformamide was added to the round bottom flask and the solution was heated to 85 ºC. Then, 5 mL of ammonium hydroxide was added to the solution, followed by an hour of vigorous stirring at 85 ºC. The curcumin coated magnetic nanoparticles (CMNPs) were washed three times with DI water and lyophilized for three days. Non-coated MNPs were synthesized in the same manner excluding the curcumin step.

2.1.2 Characterization of Curcumin-coated and Non-Coated MNPs

Transmission electron microscopy (TEM, Titan Themis 300) and scanning electron microscopy (SEM; Nova NanoSEM450, FEI) with the attached detector for energy dispersive X-ray spectroscopy (EDS; X-Max 50 silicon drift detector) were used to determine the surface morphology and elemental composition of the CMNPs and MNPs. TEM characterization was performed at 120 kV. For SEM and EDS, CMNPs and MNPs were mounted on individual SEM pin mounts with copper tape (3M, 1182). An acceleration

voltage of 10 kV and Everhart-Thornley secondary electron detector was used for SEM imaging, and an acceleration voltage of 20 kV and EDS detector was used for elemental composition analysis. ImageJ software was used to determine the ferret diameter of the nanoparticles, with the assumption that the nanoparticles are spherical. X-ray diffraction (XRD; Empyrean PANalytical) was used to analyze the crystal structure of CMNPs, MNPs, and a reference curcumin sample at 45kV and 40 mA with a 0.02 degree step size. The XRD spectrums were then compared against a library using the HighScore software (PANalytical) to confirm phase identification.

2.1.3 Magnetic Response of CMNPs and MNPs

To study therapy localization an external magnetic field, induced by a N42 neodymium magnet (#DEX0, K&J Magnetics, Inc., Pipersville, PA) with a diameter of 22 mm and a height of 25 mm was used to test the magnetic response of the CMNPs and MNPs. Specifically, 3mg of nanoparticles were weighed and dispersed in 2 mL of DI water in a 15mL conical tube. A magnet was placed on the outside surface of the tube, the minimal distance required for a magnetic response was recorded as well as the time needed to collect the dispersed nanoparticles.

2.1.4 Curcumin Release from Nanoparticles

CMNPs, MNPs, and C were incubated in simulated body fluid (rSBF). The rSBF is a solution designed to have the same ionic concentration as human blood plasma, containing Na^+(142.0 mM), K^+ (5.0 mM), Mg^{2+} (1.5 mM), Ca^{2+} (2.5 mM), Cl^- (103 mM), HCO_3^- (27 mM), HPO_4^{2-}(1.0 mM), and SO_4^{2-} (0.5 mM) ions for 9 days in triplicate. Each day rSBF was collected to determine curcumin release. The rSBF was replaced daily into

samples wells. Absorbance of curcumin was determined at 420 nm (TECAN 200 Pro, Switzerland). For cumulative release quantification, absorbance readings from prior days were added.

2.1.5 BMSC Culture

The protocol for harvesting BMSCs was approved by the Institutional Animal Care and Use Committee (IACUC) at the University of California, Riverside and has been previously established in Liu Lab at University of California, Riverside. BMSCs were harvested from the bone marrow of the femur and tibia of 14-day-old Sprague-Dawley rats. Bone marrow was flushed out by Dulbecco's Modified Eagle Media (DMEM, #SLBC9050, high glucose, D5648, Sigma-Aldrich, St. Louis, MO) supplemented with 10% fetal bovine serum and 1% penicillin/streptomycin after the distal and proximal ends of harvested bones were removed. The bone marrow and DMEM are collected and filtered through a 70 mm nylon strainer (#22363548, Thermo Fisher Scientific, Inc., Waltham, MA) to isolate harvested bone marrow stromal cells. The filtered cells were then cultured and expanded in DMEM under standard cell culture conditions (i.e., 37 °C, 5% CO_2/95% air, humidified, sterile environment) to 90% confluence [13].

Prior to cell culture 100 μg/ml, 200 μg/ml, 500 μg/ml, and 1000 μg/ml of CMNPs, MNPs, and C were sterilized by UV irradiation (M-2036, Meishida) for 30 minutes. Upon 80-90% BMSC confluence, adhered cells were washed with PBS and then detached from culture flasks using trypsin (#25200-056, Life Technologies, Carlsbad, CA). Trypsinized BMSCs were collected from each flask and centrifuged, in 15-mL

conical tubes, for 5 minutes at 1000 rpm. The supernatant was removed from the flask and the BMSCs were suspended in fresh media. To achieve a cell seeding density of 10,000 cells/cm^2, 10 μL of cell suspension was mixed with 10 μL of trypan blue (#T8154, Sigma-Aldrich, St. Louis, MO) and cells were counted using a hemocytometer (#1475, Reichert Bright-Line, Hausser Scientific, Horsham, PA). Based on cell count, the volume of cell suspension was diluted with fresh DMEM to achieve the desired cell density. To mimic how established cells may respond to the experimental nanoparticles , a direct exposure culture was done [18]. Briefly, 2 mL of the new cell suspension was pipetted into each well of a 24-well plate and cultured for 36 hours until the BMSCs formed a monolayer in each well. The culture plates were placed in an incubator under standard cell culture conditions. After 36 hours DMEM and non-adhered cells were removed from each well and replaced with fresh media and nanoparticles. A 24 hour cytocompatibility study was done with nanoparticle samples. After 24 hours media was collected and nanoparticles were removed, adhered cells were fixed with 4% paraformaldehyde (PFA; #15714-S, Electron Microscopy Science, Hatfield, PA) solution and stained with Alexa Flour 488 Phalloidin (#A12379, Life Technologies, Carlsbad, CA) for F-actin and 4′,6-diamidino-2-phenylindole (DAPI; #D3571, Life Technologies, Carlsbad, CA) for cell nuclei. Once adhered cells were fixed and stained they were imaged using a fluorescence microscope (Nikon, Ti-S eclipse, Nikon, Japan). Images were merged using ImageJ and cell adhesion density (cells/cm^2) was counted by choosing 10 random spots in each well and counting the number of cells. The number of cells was averaged and divided by the area of the image to obtain cell density.

2.2 Hyaluronic Acid Hydrogels Loaded with Curcumin-coated Magnetic Nanoparticles

2.2.1 Synthesis Magnetic Hyaluronic Acid Hydrogel

The magnetic hyaluronic acid hydrogel was synthesized through a modified chemical crosslinking protocol which was previously established [6]. Briefly, 75 mg hyaluronic acid (Bulk Supplements, Henderson, NV) and 9 mg CMNPs, MNPs, or curcumin were added to 1.425 mL water and mixed until the solution was homogenous. Immediately after, 1-ethyl-3-(3-(dimethylamino)propyl)- carbodiimide·HCl (EDC·HCl, herein referred as EDC, #22980, Thermo Fisher Scientific Inc., Waltham, MA) and N-Hydroxysuccinimide (NHS, #24500, Thermo Fisher Scientific Inc., Waltham, MA) were added to solution and mixed to induce crosslinking. To ensure homogenous mixing, the solutions were vortexed, sonicated (Qsonica, Q125, 10 minutes, pulse 5s/5s) to improve dispersion, and speed mixed (DAC 150.1 FVZ-K, FlackTek, Inc.) for 10 minutes at 3500 rpm. The resulting gel was then placed into the wells (5.5mm in diameter, and 5mm in height) of a silicone mold which had been 3D-printed (3D Bioplotter, EnvisionTEC). Samples were then left at room temperature (23 ºC) in 85% humidity overnight.

2.2.2 Hydrogel Swelling and Degradation

Hydrogel swelling was evaluated in revised simulated body fluid (rSBF). The rSBF is a solution designed to have the same ionic concentration as human blood plasma, containing Na^+(142.0 mM), K^+ (5.0 mM), Mg^{2+} (1.5 mM), Ca^{2+} (2.5 mM), Cl^- (103 mM), HCO_3^- (27 mM), HPO_4^{2-}(1.0 mM), and SO_4^{2-} (0.5 mM) ions. The hydrogels were placed

into wells of a 24-well plate with 1 mL of rSBF and incubated for 2 weeks in standard cell culture conditions (37 ºC, 5% CO_2, with humidity). Every 24 hours, the diameter, height, dry mass, buoyant mass, and density was recorded for all gels until the end of the 2 weeks. The diameter and height were determined in cm using a ruler daily. Dry mass, buoyant mass, and density were determined using (Mettler Toledo, MS105DU, MSDNY54).

2.2.3 Magnetic Response Characterization

To study therapy localization an external magnetic field, induced by a N42 neodymium magnet (#DEX0, K&J Magnetics, Inc., Pipersville, PA) with a diameter of 22 mm, a height of 25 mm, pull force of 47.20, and surface field 13,200 Guass was used to test the magnetic response of the magnetic hydrogels. HyA_CMNP and HyA_MNP were allowed to swell overnight in rSBF. The gels, with a diameter of 81 mm and 76 mm respectively, were placed in a petri dish filled with DI water. The neodymium magnet was placed 5 cm away from the gel and slowly moved towards the hydrogel. Magnetic response was recorded as distance required to initiate movement towards the magnet. Hydrogels were placed in a 15 mL conical tube filled with DI water to test vertical and horizontal movement. After the hydrogel settled to the bottom of the conical tube, the magnet was used to move the hydrogel upwards, against gravity. This was done to determine the vertical movement of the hydrogel. To determine the horizontal movement, the conical tube was placed horizontally and the magnet was used to move the gel from one end of the tube to the other end. The magnetic response for both tests was recorded. The average velocity of hydrogels was evaluated by determining total time and distance of hydrogels when stimulated by the external magnet. The average acceleration was determined by

calculating the velocities at different time points. A representation of the magnetic susceptibility of the different hydrogel samples was compared to determine if any quantitative changes for changes in magnetism with distance can be determined between gels. Magnetic susceptibility is a dimensionless proportionality constant indicating the degree of magnetization of the hydrogels in response to an applied magnetic field. This was done by determining the attractive force between the magnet and hydrogel samples. The attractive susceptibility (F) was calculated by taking the product of the magnetic field strength (H) and susceptibility (X).

$$XH = \mathrm{F}$$

Magnetic field strength varies inversely with the square of the distance between the magnet and the hydrogel samples:

$$\frac{H0}{r^2} = H$$

*H0 is a constant that characterizes the strength of the magnet by itself.

After incorporating this into the equation for attractive susceptibility, the equation becomes:

$$\frac{X\ H0}{r^2} = F = ma$$

Given the mass of the hydrogel samples are approximately equal the susceptibility can be calculated by:

$$F = a\ r^2$$

The velocities and accelerations of hydrogel samples were calculated by the following equations:

$$\frac{\Delta\, \boldsymbol{Distance}\ (\boldsymbol{m})}{\Delta\, \boldsymbol{Time}\ (\boldsymbol{s})} = \boldsymbol{Average\ Velocity}\ (\boldsymbol{m/s}\ \ )$$

$$\frac{\Delta\, \boldsymbol{Velocity}\ (\boldsymbol{m/s})}{\Delta\, \boldsymbol{Time}\ (\boldsymbol{s})} = \boldsymbol{Average\ Acceleration}\ (\boldsymbol{m/s^2})$$

2.2.4 Sample Sterilization and BMSC Culture

Cytocompatibility of hydrogels and nanoparticles controls were done via a direct exposure culture, as described for the nanoparticle study in section 2.1.5. Cells were harvested, and diluted as previously described. Prior to cell culture, hydrogels and nanoparticles were sterilized by UV irradiation (M-2036, Meishida) for 30 minutes. Briefly, 2 mL of the new cell suspension was pipetted into each well of a 24-well plate and cultured for 36 hours until the BMSCs formed a monolayer in each well. The culture plates were placed in an incubator under standard cell culture conditions. After 36 hours DMEM and non-adhered cells were removed from each well and replaced with fresh media. Instead of different concentrations of nanoparticles, sterilized HyA_CMNP, HyA_MNP, HyA_C, HyA, CMNPs, MNPs, C were added into the respective wells. 1 mg of CMNPs, MNPs, and C were added to the wells as controls for the amount of nanoparticles present in each gel. Cells were fixed, stained, and imaged as they were in 2.1.5. Cell density was also calculated in the same way.

2.2.5 Post-Culture Media Analysis

Post-culture media was analyzed by quantifying pH, Fe^{2+} and Ca^{2+} concentration, and total curcumin release. The pH of the post-culture media was measured using a pre-calibrated pH meter (Symphony SB70P, VWR). The concentrations of Fe^{2+} and Ca^{2+} ions were measured using inductively coupled plasma optical emission spectrometry (ICP-OES; PerkinElmer Optima 8000). For the ICP-OES analysis, the collected post-culture media was first diluted to 1:100 in nitric acid, and then fed into the instrument for the measurement using an auto sampler. Concentrations of Fe^{2+} and Ca^{2+} ions were calculated based on the calibration curves generated using Fe and Ca standards (Perkin Elmer) diluted to the ranges of 0.5–5.0 and 0.1–1.0 mg/L, respectively. HyA_CMNP, HyA_MNP, HyA_C, and HyA lost integrity post culture, media and gel was collected and curcumin release absorbance was determined at 420 nm (TECAN 200 Pro, Switzerland).

2.3 VEGF Secretion Assay

BMSCs were cultured in the presence of HyA_CMNP, HyA_MNP, HyA_C, CMNPs, MNPs, and C for 48 hours. At the 48 hour time point media was collected and centrifuged for 10 minutes at 2000 rpm to remove gel and particles. The supernatant was collected and VEGF was measured by an enzyme-linked immunosorbent assay (ELISA, Boster Biological Technology, Pleasanton, CA). Adhered cells were fixed with 4% PFA (#15714-S, Electron Microscopy Science, Hatfield, PA) and stained with Alexa Flour 488 Phalloidin (#A12379, Life Technologies, Carlsbad, Ca) for F-actin and DAPI (#D3571, Life Technologies, Carlsbad, CA) for cell nuclei. Cell were imaged with a fluorescence microscope (Nikon, Ti-S eclipse, Nikon, Japan). and counted using ImageJ to quantify

cell density. The VEGF concentration was measured in picograms per milliliter. VEGF secretion per cell was calculated as

$$\frac{[\boldsymbol{VEGF\ pg/mL}]*\boldsymbol{Media\ Volume\ (mL)}}{\boldsymbol{Cell\ Density}\left(\frac{\boldsymbol{cells}}{\boldsymbol{cm^2}}\right)*\boldsymbol{Area\ of\ well}\ (\boldsymbol{cm^2})}.$$

For further analysis of VEGF release, VEGF (pg/cells) released from HyA_CMNP, HyA_MNP, HyA_C, CMNPs, MNPs, and C was divided by BMSCs only control.

$$\frac{\left[\boldsymbol{VEGF}\ (\frac{\boldsymbol{pg}}{\boldsymbol{cell}})\right]\boldsymbol{of\ sample}}{\left[\boldsymbol{VEGF}\ (\frac{\boldsymbol{pg}}{\boldsymbol{cell}})\right]\boldsymbol{of\ BMSCs\ only}}.$$

2.4 Statistical Analysis

All experiments were run in triplicate. All data sets were tested for normal distribution and homogeneous variance. Parametric data sets were analyzed using one-way analysis of variance (ANOVA) to analyze whether or know there is a difference between sample means, followed by the Tukey test to determine if the differences are significant. Statistical significance was considered at $P < 0.05$.3. Results

3.1 Characterization and Magnetic Response of C-MNPs

The CMNPs and MNPs exhibited a spherical morphology with diameters of 17 ± 5 nm and 16 ± 4 nm, respectively. This was confirmed by the scanning electron micrograph at a resolution of 40,000X (Figure 1A' Figure 1B'). The presence of carbon (C; 52 Atomic %), oxygen (O, 33 Atomic %), and iron (Fe, 15 Atomic %) was detected in CMNPs, and carbon (C, 9 Atomic %), Oxygen (O, 26 Atomic %) and iron (Fe, 62 Atomic %) was detected in MNPs by the corresponding EDS analysis (Figure 2). These results were expected based on the chemical make-up of curcumin ($C_{21}H_{20}O_6$) and iron oxide (Fe_3O_4).

For CMNP and MNP, the major XRD peaks (Figure 3) for Fe_3O_4 are present as well as the minor peaks for Fe_2O_3 spanning over a 2θ range (5–65°) that matches with JDPCS card (19-0629) confirming the presence of iron oxide. Quantitative analysis of the SEM image showed that the average size of CMNPs was 17 ± 4 nm and MNPs 17 nm ± 4 nm (Figure 1A'' Figure 1B'').

Magnetic response was determined to evaluate the potential for nanoparticles to be magnetically guided to localize treatment. Magnetic response was evaluated for dry and DI water-suspended CMNPs and MNPs (Figure 4). For dry and suspended nanoparticles, CMNPs and MNPs exhibited response to the magnet when it was at distance of 35mm and 10mm respectively. The dry CMNPs and MNPs were collected with external magnetic stimuli in 1 second, while the CMNPs in DI water were collected in 3 second and MNPs were collected in 1 second.

Absorbance readings corresponding with curcumin release at the end of 9 days for CMNPs, MNPs, and C was 0.86, 0.22, and 0.57, respectively (Figure 4). Iron oxide nanoparticles lose their magnetic ability when oxidized. Positive readings for curcumin in MNPs samples, and increased curcumin reading in CMNPs samples after day 5 can be explained by the presence of oxidized iron oxide nanoparticles present rSBF.

The morphology and adhesion of BMSCs cultured in varying concentrations of CMNPs and MNPs is shown in Figure 6. The concentrations were 0 μg/ml, 100 μg/ml, 200 μg/ml, 500 μg/ml, and 1000 μg/ml. Morphology of BMSCs were normal for concentrations of CMNPs at the concentrations evaluated. For MNPs, normal morphology was observed for up to 200 μg/ml at which point cells began to exhibit less spreading. BMSCs exposed

to curcumin showed healthy morphology with enhanced spreading up to 500 μg/ml. BMSC adhesion density when cultured with CMNPs was 7.6 x 10^3 cells/cm^2, 10.6 x 10^3 cells/cm^2, 13.4 x 10^3 cells/cm^2, 9.4 x 10^3 cells/cm^2, for 100 μg/ml, 200 μg/ml, 500 μg/ml, and 1000 μg/ml, respectively. BMSC adhesion density when cultured with MNPs was 9.8 x 10^3 cells/cm^2, 11.5 x 10^3 cells/cm^2, 12.8 x 10^3 cells/cm^2, and 11.0 x 10^3 cells/cm^2, for 100 μg/ml, 200 μg/ml, 500 μg/ml, and 1000 μg/ml, respectively. BMSC adhesion density when cultured with C was 10.8 x 10^3 cells/cm^2, 12.9 x 10^3 cells/cm^2, 8.4 x 10^3 cells/cm^2, and 4.8 x 10^3 cells/cm^2, for 100 μg/ml, 200 μg/ml, 500 μg/ml, and 1000 μg/ml, respectively. None of the samples exhibited significantly different cell density compared to the 0 μg/ml control, which had a cell density of 8.3 x 10^3 cells/cm^2. As shown in Figure 7A, wells with 500 μg/ml had more cells overall in both MNPs and C-MNPs groups and cells that were cultured with no particles had fewer adherent cells on average after the 24 hour culture. There was no significant change in pH as shown in Figures 7B.

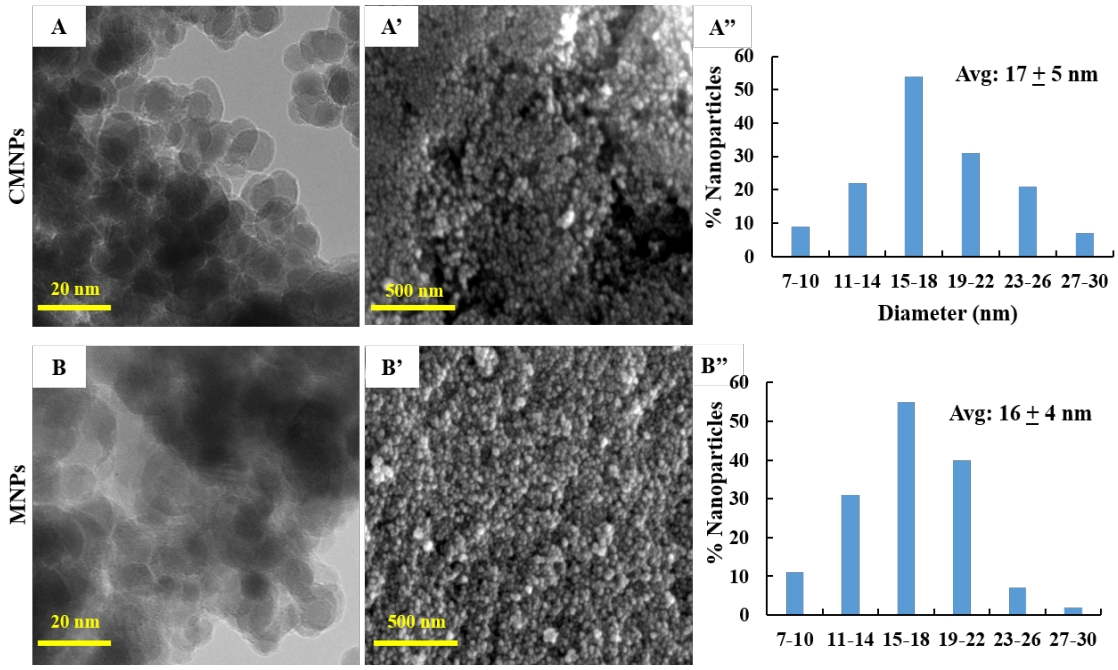

Figure 1. (A) and (B) TEM image of CMNPs and MNPs respectively, scale bar = 500 nm. Original magnification 100 000X. (A') and (B') SEM image of CMNPs and MNPs respectively, scale bar = 20 nm. Original magnification 40 000X. (A''') and (B''') Bar graph showing particle size distribution of CMNPs and MNPs. Average size of CMNPs was determined to be 17 $\pm$ 5 nm, and average size of MNPs was 16 $\pm$ 4 nm.

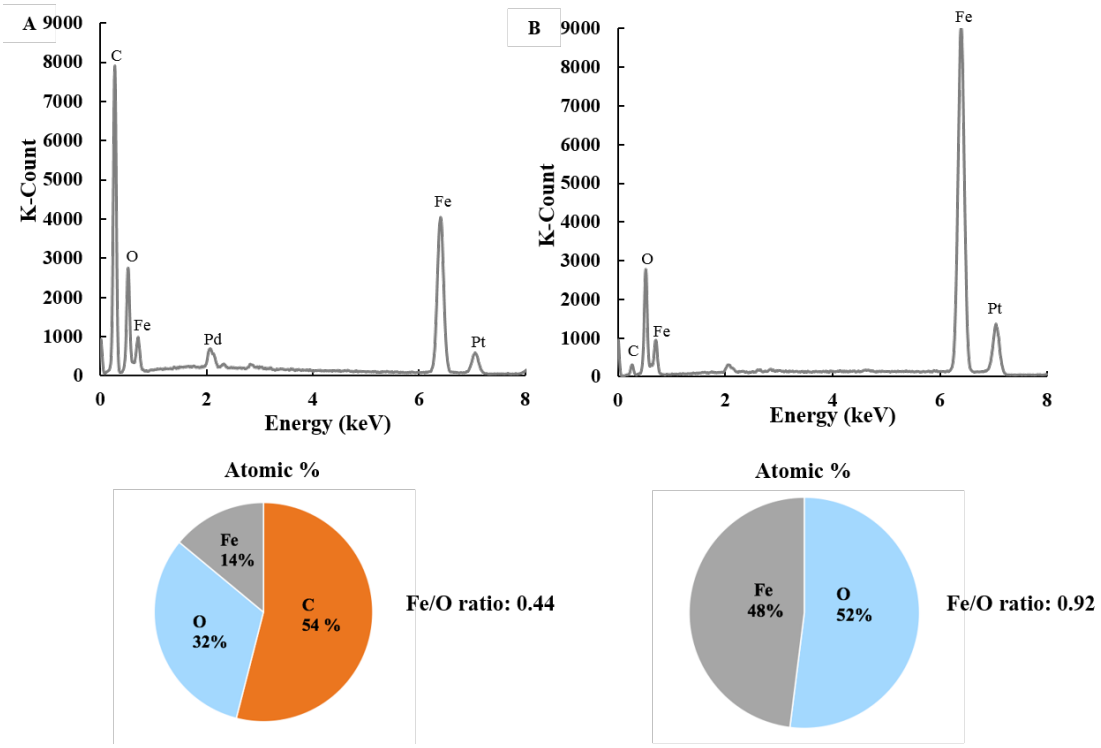

Figure 2. EDS spectrum and quantification of elemental composition of CMNPs (A) and MNPs (B) and the corresponding atomic percentage are shown in the same order.

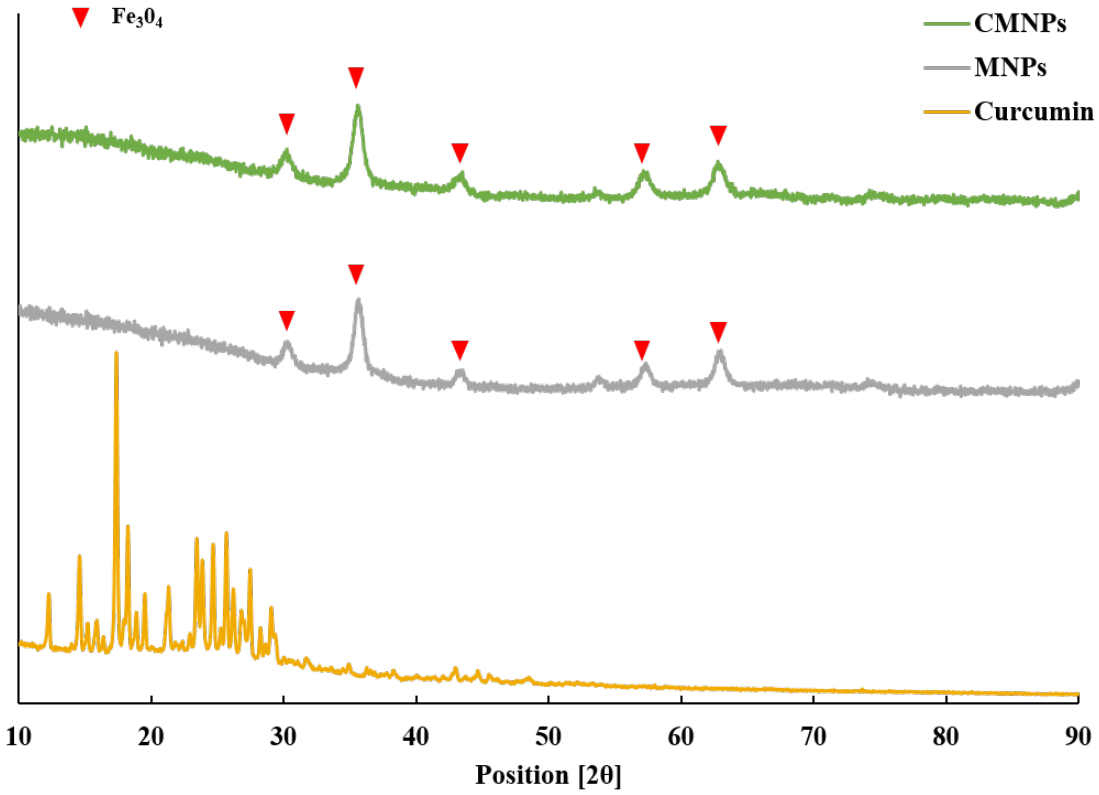

Figure 3. (A)XRD spectrum of C-MNPs (top), MNPs (middle), and curcumin (bottom).

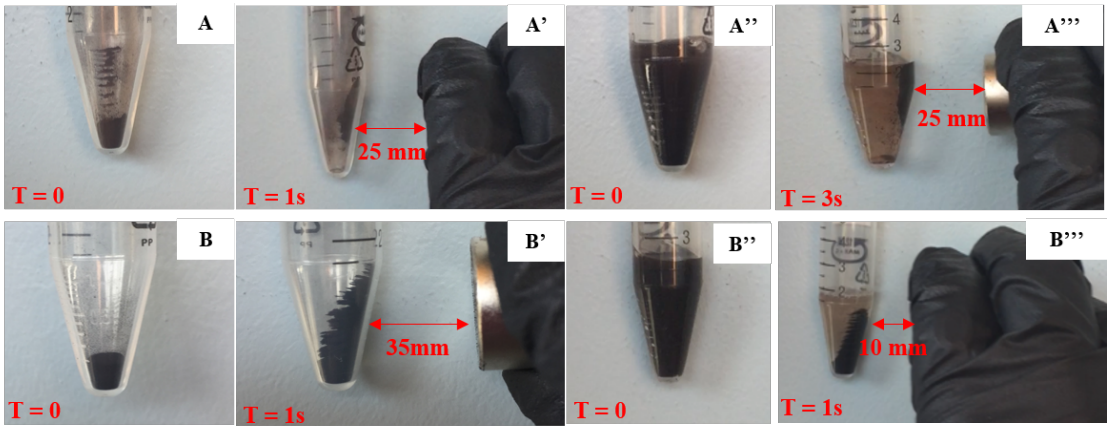

Figure 4. Magnetic response to MNPs and CMNPs. (A) showing CMNPs before eternal magnet stimulated, (A'') showing CMNPs response to magnetic stimulated, (A'') CMNPs dispersed in DI water before magnetic stimulation (A''') CMNPs dispersed in DI water after magnetic stimulation. (B) shows MNPs before eternal magnet stimulated, (B'') showing MNPs response to magnetic stimulated, (B'') MNPs dispersed in DI water before magnetic stimulation (B''') MNPs dispersed in DI water after magnetic stimulation. Dry CMNPs responded at after 1 second of magnetic stimulation at a minimum distance of 25 mm. CMNPs in water responded to magnetic stimulation after 3 seconds of magnetic stimulation at a minimum distance of 25mm. Dry MNPs responded after 1 second at a minimum distance of 35 mm, and after 1 second and at a minimum distance of 10mm in water.

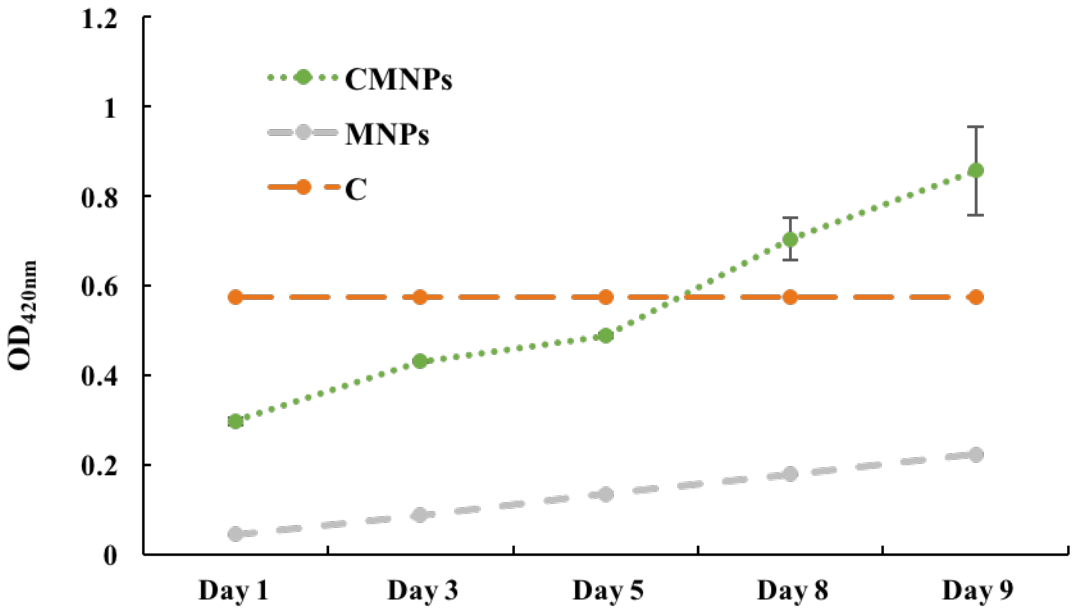

Figure 5: Cumulative curcumin release over 9 days presented in absorbance at 420 nm as well as the corresponding curcumin concentration based on a calibration curve. Initial curcumin concentration is represented in orange, cumulative curcumin release from CMNPs and MNPs is represented in green and grey respectively.

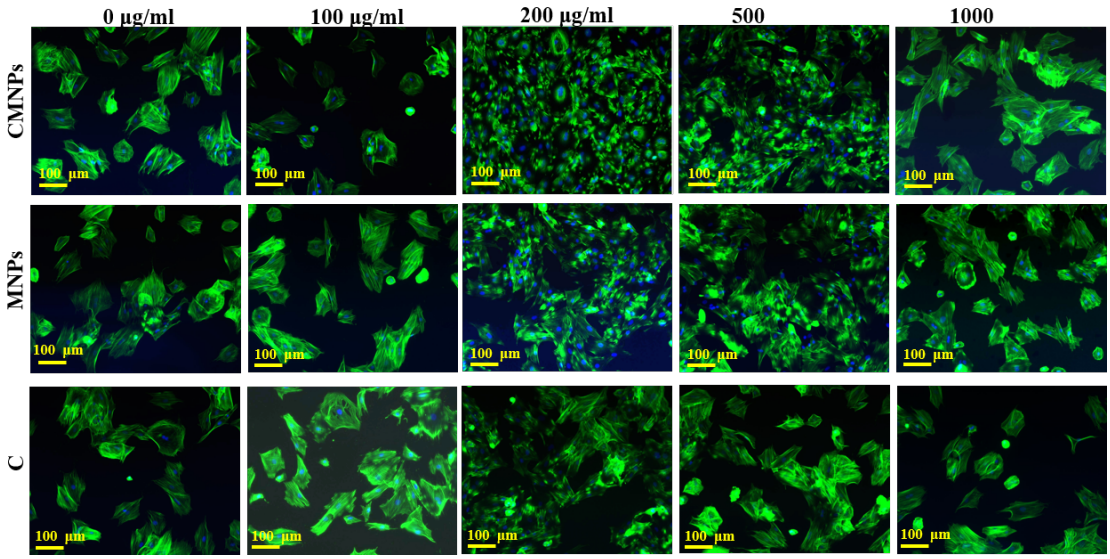

Figure 6. Fluorescence images of BMSC adhesion and morphology when cultured with CMNPs, C, and MNPs in varying concentrations. Row A shows images of BMSCs culture in 0 µg/ml, 100 µg/ml, 200 µg/ml, 500 µg/ml, and 1000 µg/ml MNPs respectively. Row B shows images of BMSCs culture in 0 µg/ml, 100 µg/ml, 200 µg/ml, 500 µg/ml, and 1000 µg/ml CMNPs respectively. F-actin of the BMSCs is stained green and nuclei are stained blue. Scale bar = 100nm.

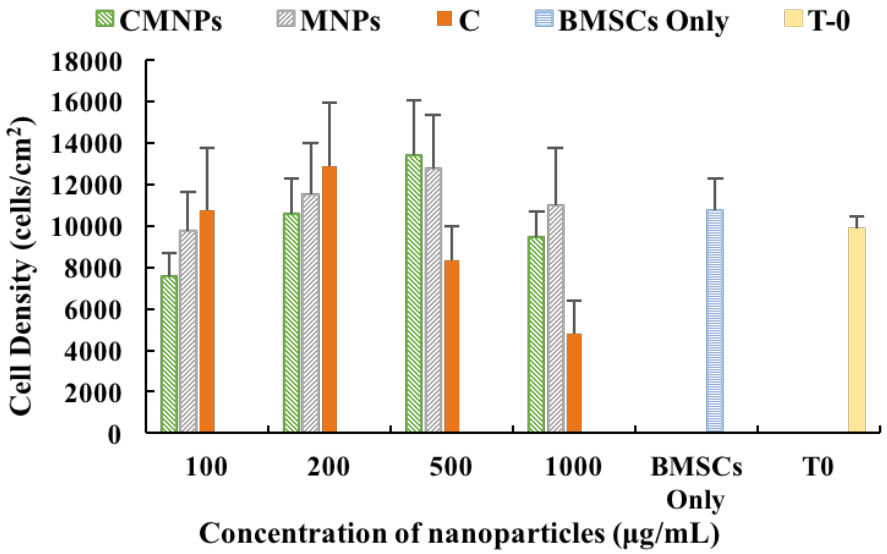

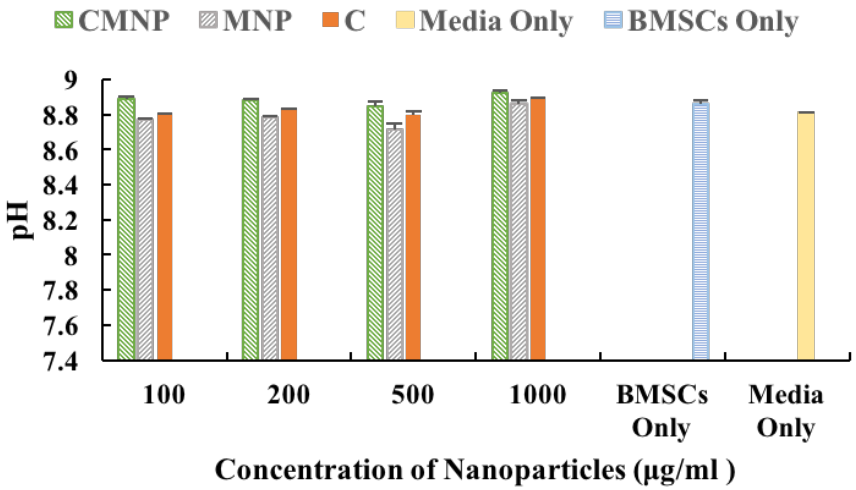

Figure 7. (A) Cell density for each experimental group of 24 hour toxicity study. From left to right: BMSCs cultured 100 µg/ml CMNPs (green), MNPs (gray), and C (orange) concentration, 200 µg/ml CMNPs (green), MNPs (gray), and C (orange) concentration, 500 µg/ml CMNPs (green), MNPs (gray), and C (orange) concentration, 1000 µg/ml CMNPs (green), MNPs (gray), and C (orange) concentration, BMSCs Only and Media Only. Values are mean ± standard error. (B) Post-culture media pH values of 24 hour toxicity study. From left to right: BMSCs cultured 100 µg/ml CMNPs (green), MNPs (gray), and C (orange) concentration, 200 µg/ml CMNPs (green), MNPs (gray), and C (orange) concentration, 500 µg/ml CMNPs (green), MNPs (gray), and C (orange) concentration, 1000 µg/ml CMNPs (green), MNPs (gray), and C (orange) concentration, BMSCs Only and Media Only. Values are mean ± standard error.

3.2 Characterization and Magnetic Response of Magnetic Hydrogel

Gel samples retained the cylindrical shape of the molds they were placed in after incubation in 80% humidity overnight. Prior to submersion in rSBF, HyA_CMNP is dark brown in color. The HyA_MNP sample is also brown, but it is slightly lighter than HyA_CMNP, which may indicate that the MNPs in HyA_MNP have slightly oxidized as shown in Figure 8. As expected, HyA_C is orange in color, which is indicative of the presence of curcumin. When incubated in rSBF the gels absorbed the solution and swelled (increasing in height and diameter). Prior to submersion, the starting diameter of each hydrogel was 5.5 mm. After 24 hours of submersion, the diameters of HyA_CMNP, HyA_MNP, HyA_C, and HyA were 25 mm, 20 mm, 22 mm, and 21 mm, respectively. After 9 days, the gel colors changed to lighter brown and semi-transparent for HyA_CMNP and HyA_MNP, respectively. At the 9 day point, the diameters of HyA_CMNP, HyA_MNP, HyA_C, and HyA increased to 26 mm, 23 mm, 24 mm, and 22 mm, respectively. The mass change and volume over time confirmed the absorption of fluid. The HyA_CMNP gel lost structural integrity after 14 days, HyA_MNP after 9 days, HyA_C after 14 days, and HyA after 14 days. The mass of HyA_CMNP changed from 65 mg to 628 mg, HyA_MNP changed from 65 mg to 426 mg, HyA_C changed from 68 mg to 546 mg, and HyA changed from 64 mg to 419 mg. All gels had a density close to 1 by day 3 of incubation. The changes in gel volume, mass, buoyant mass, and density are shown in Figure 9.

Magnetic response was determined to evaluate the potential for hydrogels to be magnetically guided to localize treatment. HyA_CMNP showed magnetic response when

it was exposed to an external magnet 42.5 mm away (Figure 9A''), while HyA_MNP showed magnetic response when it was exposed to an external magnet 22.5 mm away (Figure B''). The magnetic response was also evaluated 1 day after incubation in rSBF, the minimal distance for magnetic response for HyA_CMNP was still 32.5 mm but 12 mm for HyA_MNP. In both cases, the hydrogel took about 1s to start movement towards the magnet. HyA_CMNP travelled 42.5 mm in 3.91 seconds while HyA_MNP travelled 32.5 mm in 3.17 seconds implying before incubation while HyA_CMNP travelled 22.5 cm in 6.36 seconds and HyA_MNP travelled 12 mm in .81 second one day after incubation in rSBF. The natural velocities of the magnetic gel movement are 10.87 mm/s and 10.25 mm/s respectively before incubation and 3.54 m/s and 14.8 m/s after one day of incubation respectively. However, the speeds could be adjusted by moving the magnet away from the gel quickly. The results of the vertical and horizontal magnetic response tests show that the HyA_CMNP and HyA_MNP gels can both be moved against gravity and can move in the same direction as the magnet is moved horizontally. Instantaneous acceleration of the hydrogel samples with distance was calculated as the following for HyA_CMNP:

HyA_CMNP Day 0		HyA_CMNP Day 1	
Distance from magnet (mm)	Acceleration (m/s^2)	Distance from magnet(mm)	Acceleration(m/s^2)
35	4.671338005		
30	7.807363577	22.5	11.19463743
25	52.71193835	17.5	18.85740522
20	59.44293478	12.5	58.75933854
15	187.5	7.5	93.42883837
10	555.5555556	2.5	747.8632479
0	1484.230056	0	2083.333333

Instantaneous acceleration of the hydrogel samples with distance was calculated as the following for HyA_MNP:

HyA_MNP Day 0		HyA_MNP Day 1	
Distance from magnet (mm)	Acceleration (m/s^2)	Distance from magnet (mm)	Acceleration (m/s^2)
15	0.351148464		
10	21.7388073		
5	1041.666667	8	1155.408455
0	1199.494949	0	1200

Magnetic susceptibility for hydrogel samples was calculated as the following: HyA_CMNP Day 0 has a magnetic susceptibility of 27,869, HyA_CMNP Day 1 has a magnetic susceptibility of 6,110, HyA_MNP Day 0 has a magnetic susceptibility of 10, 746, and HyA_MNP Day 1 has a magnetic susceptibility of 1,177.

3.2.1 BMSC Viability when cultured with Hydrogels and Nanoparticles

After the 48 hours study, HyA_CMNP completely lost structural integrity, HyA_MNP maintained structural integrity and swelled up with DMEM fluid, filling the well. HyA_C partially lost structural integrity but was intact enough to remove from the culture well. HyA also maintained structural integrity and swelled up with DMEM to fill the well. Due to the loss of some samples, cells were unable to be imaged on the sample itself. BMSCs adhered on the culture wells in each sample were imaged to determine cytocompatibility with gels.

Morphology of BMSCs varied between different hydrogel samples (Figure 11). BMSCs are elongated, more spread out, and more interconnected in the presence of HyA_CMNP compared to HyA_MNP, HyA_C, HyA. BMSCs in the presence of

HyA_MNP and HyA are less spread out and have a circular morphology compared to the elongation of the previously described BMSCs. Similarly, in nanoparticle samples cells that are in the presence of CMNPs and C are more elongated and spread out compared to the cultured with MNPs.

BMSC cell density in each well was quantified (Figure 12). Overall HyA_CMNP showed the higher average cell density. Specifically, cell density after exposure to HyA_CMNP, HyA_MNP, HyA_C, and HyA was 2.5 x 10^3 cells/cm^2, 1.5 x 10^3 cells/cm^2, 1.7 x 10^3 cells/cm^2, and 1.0 x 10^3 cells/cm^2, respectively. The cell density after exposure to CMNP, MNPs, and C was 6.1 x 10^3 cells/cm^2, 5.7 x 10^3 cells/cm^2, and 4.6 x 10^3 cells/cm^2, respectively. The control well of BMSCs only yielded a cell density of 4.0 x 10^3 cells/cm^2. HyA_CMNP showed significant results when compared to HyA_C and BMSCs only controls.

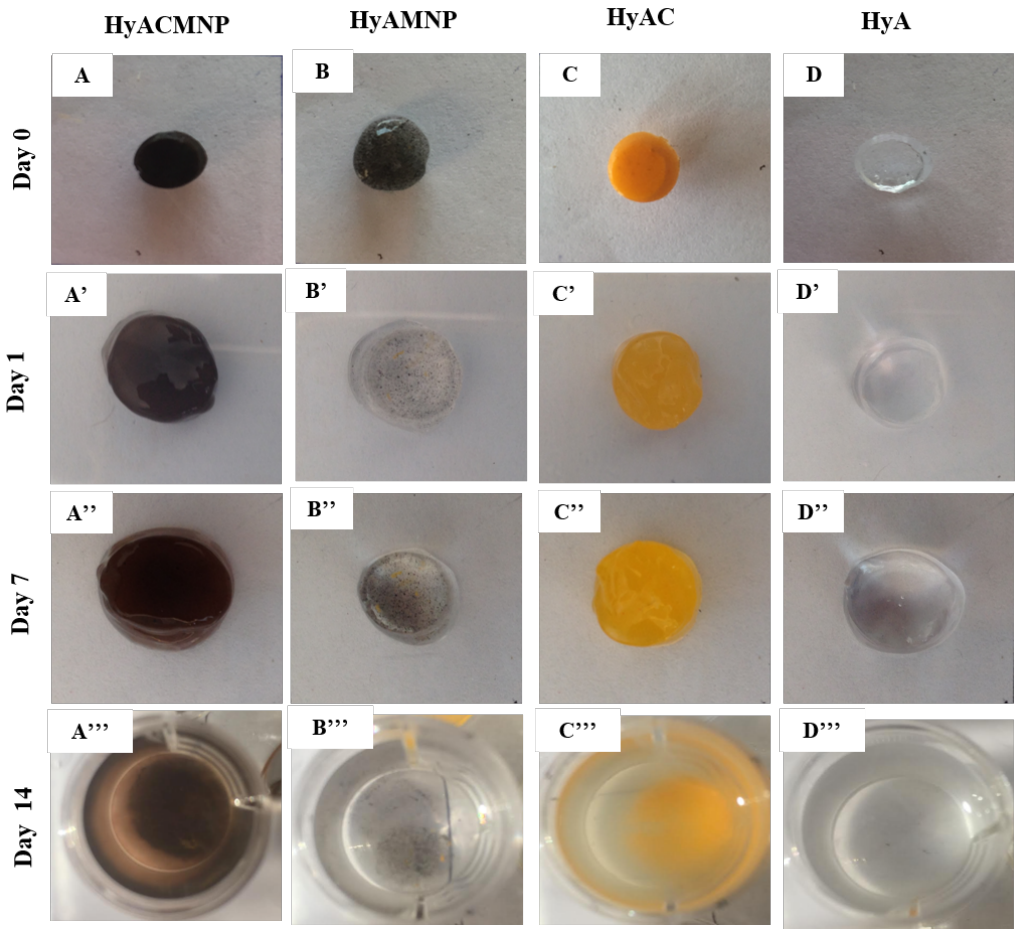

Figures 8: HyA_CMNP (A), HyA_MNP (B), HyA_C (C), and HyA (D) gels before incubation in rSBF HyA_CMNP (A'), HyA_MNP (B'), HyA_C (C'), and HyA (D') gels one day after incubation in rSBF HyA_CMNP (A''), HyA_MNP (B''), HyA_C (C''), and HyA (D') 7 days after incubation in rSBF. HyA_CMNP (A''), HyA_MNP (B'''), HyA_C (C'''), and HyA (D''') 14 days after incubation in rSBF.

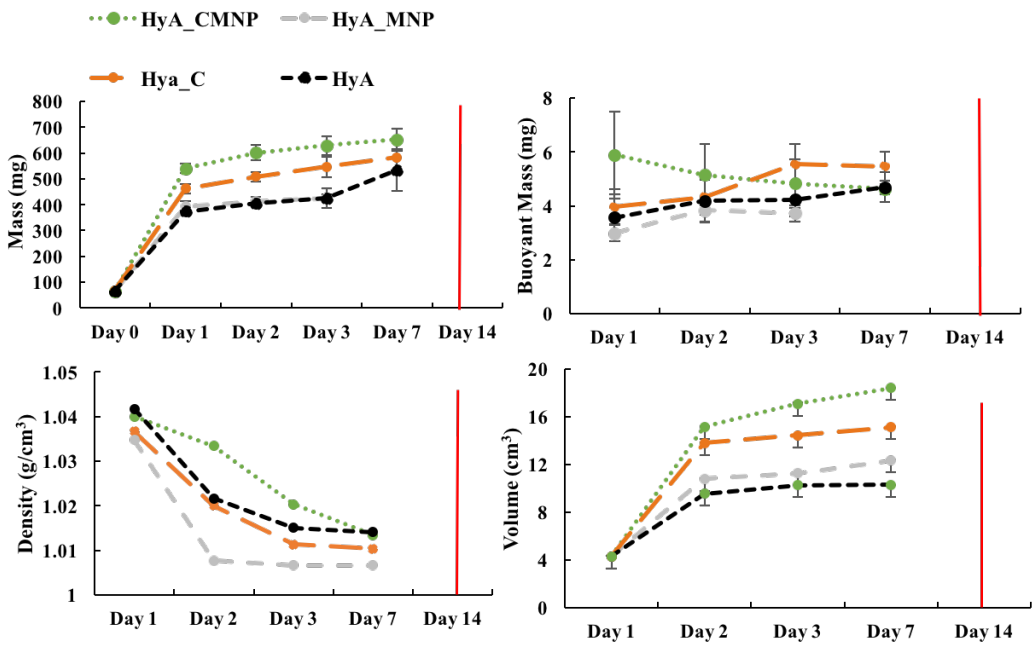

Figure 9. (A) diameter, (B) dry mass, (C) density, (D), and wet mass change of HyA_CMNP (green), HyA_MNP (gray), HyA_C (orange), and HyA (black) over the span of two weeks. HyA_MNP lost integrity after 9 days, and HyA_CMNP, HyA_MNP, HyA_C lost integrity after 14 days.

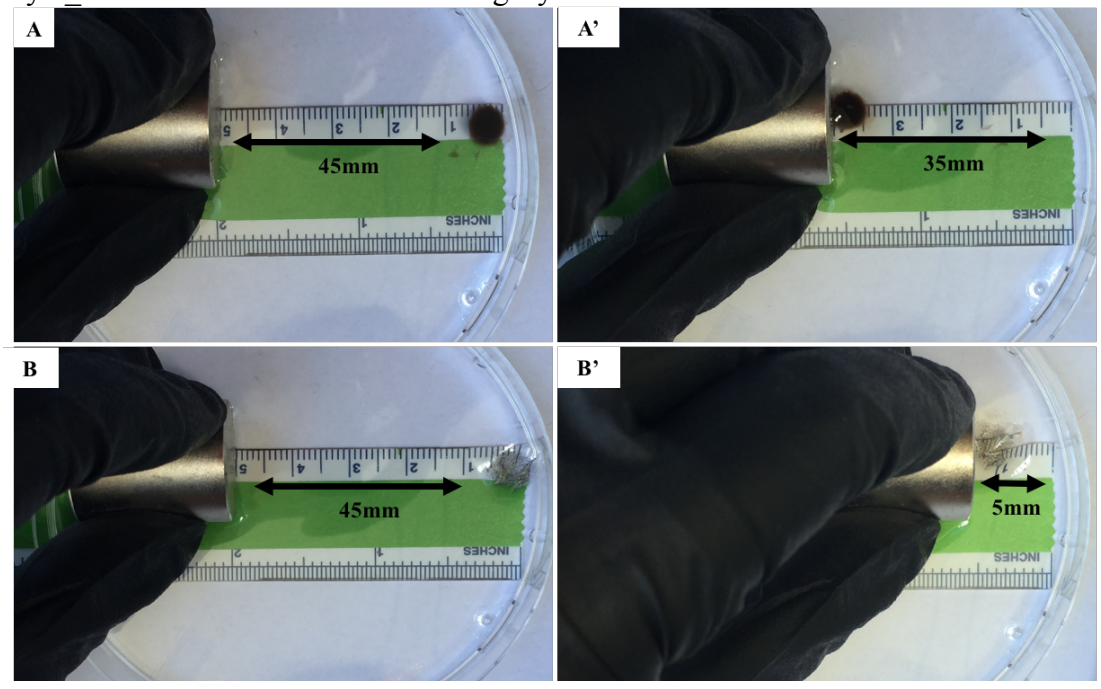

Figure 10: Magnetic response of HyA_CMNP (A and A') and HyA_MNP (B and B') in DI water one day after incubation in rSBF. Magnetic response of HyA_CMNP was detected at a minimum of 35mm and 5mm from HyA_MNP.

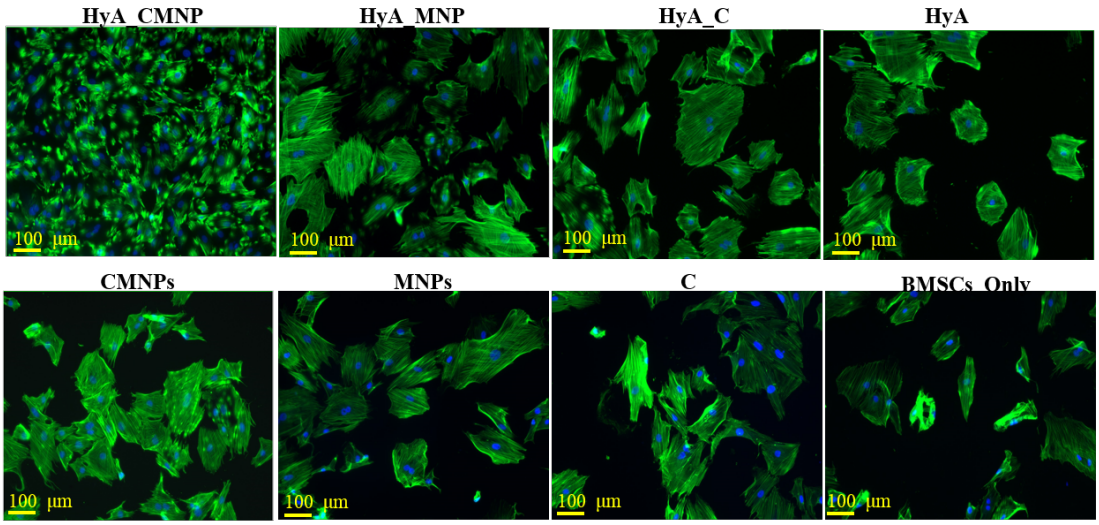

Figure 11: Fluorescence images of BMSC adhesion and morphology for each experimental group of samples after a 24 hour culture. From left to right: HyA_CMNP, HyA_MNP, HyA_C, HyA, CMNPs, MNPs, C, Cells Only.

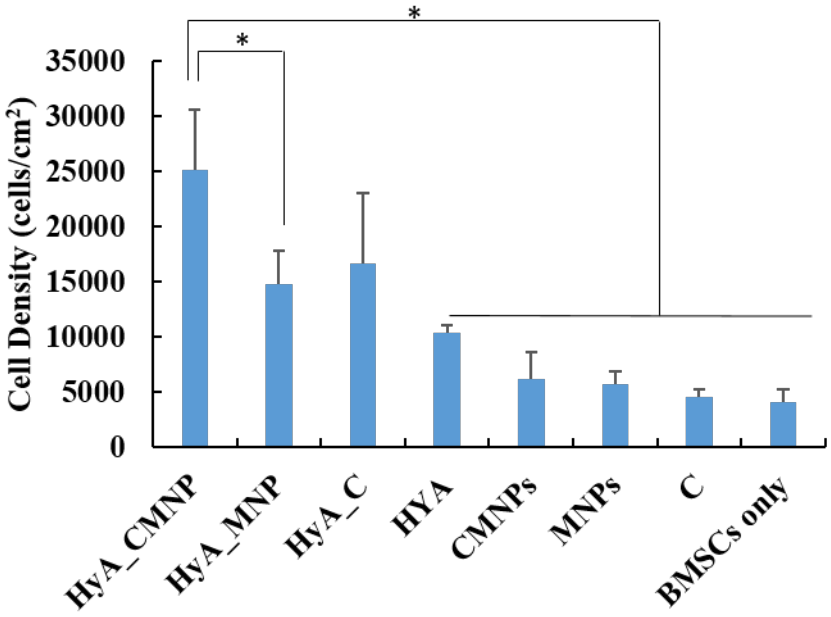

Figure 12: Cell density for each experimental group of 24 hour toxicity study. From left to right: BMSCs cultured with: HyA-C-MNPs, HyA-MNP,s HyA-C, HyA, C-MNPs, MNPs, and cells only. Values are mean ± standard error. Significant results were seen between HyA_CMNP compared with HyA_C and BMSCs. *p≤0.05

3.2.2 Post-Culture Media Analysis

Absorbance measurements corresponding to total curcumin released after cell culture from HyA_CMNP, HyA_MNP, HyA_C, HyA, CMNPs, MNPs, C, BMSCs only, and Media control were 0.401 ± 0.069, 0.077 ± 0.002, 0.434 ± 0.069, 0.082 ± 0.002, 0.072 ± 0.002, 0.104 ± 0.010, 0.498 ± 0.287, 0.075 ± 0.0004, and 0.104 ± 0.009, respectively (Figure 13B). HyA_CMNP, HyA_C, and C all had significantly greater absorbance compared to all other samples. This is due to the release of curcumin, which was absent in other samples.

The post-culture pH remained between 8.1 and 8.3 for all samples (Figure 13A). While the growth of BMSCs raised pH in the BMSC control when compared to the Media control, this increase was not statistically significant. Therefore, most of the change in pH was likely from the materials, rather than cell growth. However, as the increase was minimal and well-within the buffering capabilities of bicarbonate, it is unlikely that this affected cell growth.

Free Fe^{2+} ion concentration was measured to determine if iron oxide in the materials released ions (Figure 13C). The Fe^{2+} concentration was between 0.01 mM and 0.04 mM for all experimental samples. All experimental samples, as well as BMSCs only, showed increase in Fe^{2+} concentration with respect to the media only control, which had a Fe^{2+} concentration less than .01 mM. This is likely due to normal metabolism of Fe^{2+} within media by the BMSCs. In general, the concentration of Fe^{2+} is low in all samples, with only a significant increase in the HyA_MNP sample which could indicate the release of Fe^{2+} from nanoparticles.

Calcium is an essential nutrient to bone healing, and as we are interested in angiogenesis in bone tissue, free Ca^{2+} concentration in the media was also measured (Figure 13D). For all conditions, Ca^{2+} concentration was between 1.27 mM and 2.3 mM. HyA_CMNP resulted in a media Ca^{2+} concentration of 1.74 mM, which was statistically lower than the Media control with a Ca^{2+} concentration of 2.25 mM. This is likely due to normal cell metabolism of Ca^{2+}.

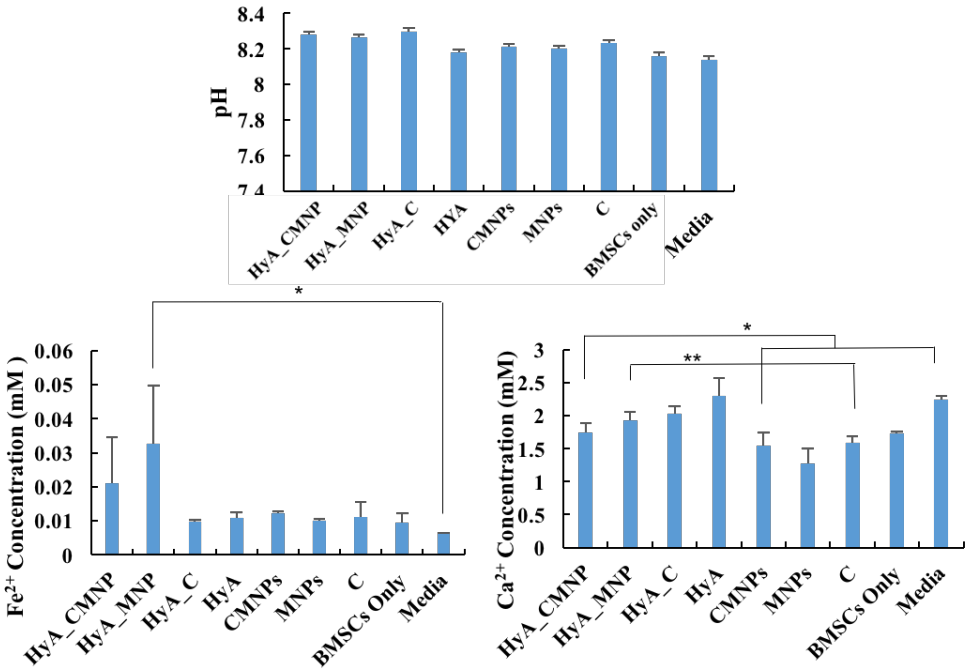

Figure 13. Post culture media analysis done by (A) pH quantification, (B) Fe^{2+} Concentration determination, and (C) Ca^{2+} Concentration (mM) determination after BMSCs were cultured with HyA_CMNP, HyA_MNP, HyA_C, CMNPs, MNPs, C for 24 hours. *$p \leq 0.05$, **$p \leq 0.005$

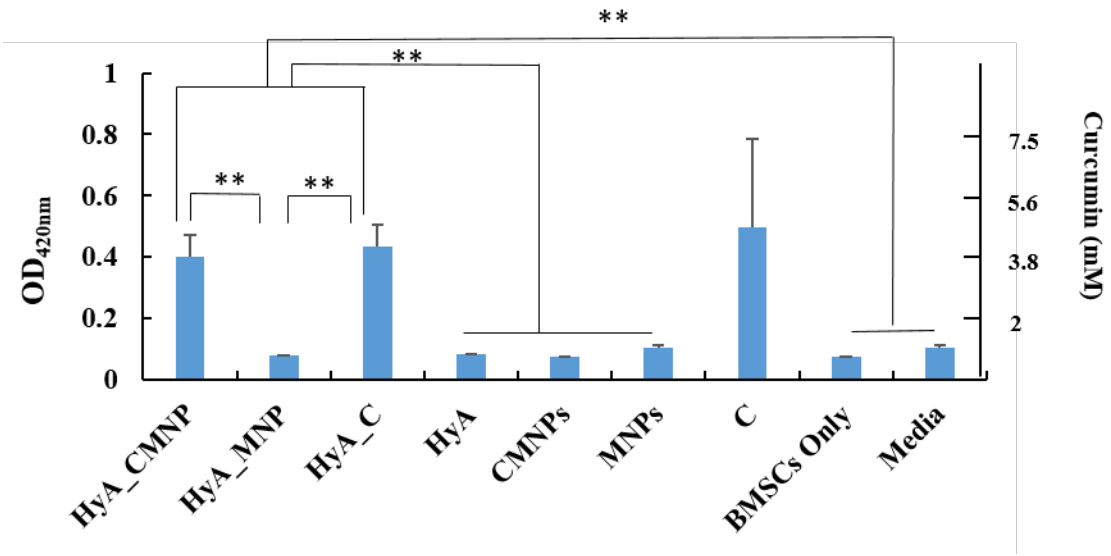

Figure 14. Post culture curcumin release after HyA_CMNP, HyA_MNP, HyA_C, HyA, CMNPs, MNPs, C was cultured with BMSCs for 24 hours. Curcumin release absorbance was determined at 420 nm and corresponding curcumin concentration was based on a calibration curve. **$p \leq 0.005$

3.3 VEGF Secretion by BMSCs exposed to Hydrogels

VEGF secretion was quantified as VEGF concentration and VEGF secretion per cell (Figure 15B and Figure 16). Total VEGF concentration after exposure to HyA_CMNP, HyA_MNP, HyA_C, and HyA, CMNPs, MNPs, C, BMSCs Only was 2055 pg/mL, 447pg/mL, 1119 pg/mL, 771pg/mL, 809 pg/mL, 847 pg/mL, 1869 pg/mL, 1314 pg/mL, respectively. HyA_CMNP had the highest average VEGF concentration and was statistically significant to HyA_MNP, HyA_C, HyA, CMNPs, and MNPs. When normalized as VEGF/cell, trends changed due to difference in cell density. HyA_CMNP, HyA_MNP, HyA_C, HyA, CMNPs, MNPs, C, and BMSCs Only showed VEGF secretion by cell was 0.36 pg/cell, 0.26 pg/cell, 0.56 pg/cell, 0.34 pg/cell, 0.15 pg/cell, 0.78 pg/cell, and 0.59 pg/cell, respectively. In terms of magnetic nanoparticles, cell secreted more

VEGF when curcumin was involved, while samples with just MNP secreted the least amount of VEGF detected.

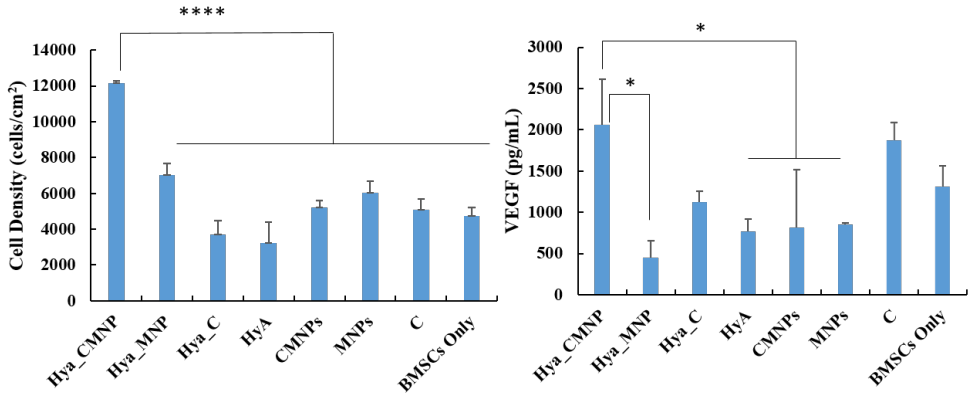

Figure 15. VEGF secretion determined by an ELISA assay from collected media after a 48 hours cell culture. Cells were cultured in the presence of the following samples, from left to right: HyA_CMNP, HyA_MNP, HyA_C, HyA, CMNPs, MNPs, C, cells Only. Cell density was determined and VEGF secretion was normalized from pg/mL to pg/cell. Total volume of media was 2.5mL, total area of cell culture well was 1.9 cm^2. *$p \leq 0.05$, ****$p \leq 0.0005$

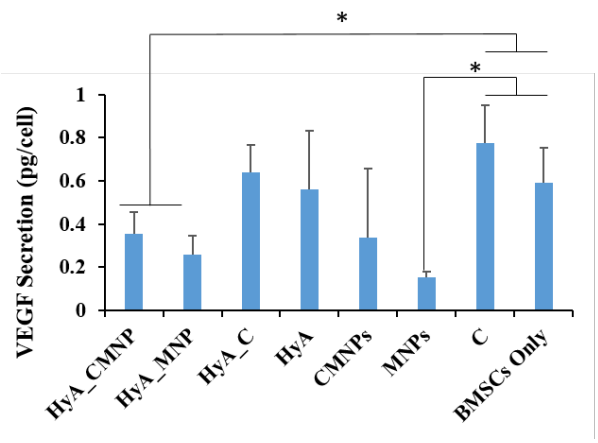

VEGF Release Ratio Compared to BMSCS Control	
HyA_CMNP	0.607768179
HyA_MNP	0.229245479
HyA_C	1.085253604
HyA	0.856895629
CMNPs	0.559277575
MNPs	0.506475249
C	1.31830394

Figure 16. VEGF secretion determined by an ELISA assay from collected media after a 48 hours cell culture. Cells were cultured in the presence of the following samples, from left to right: HyA_CMNP, HyA_MNP, HyA_C, HyA, CMNPs, MNPs, C, cells only. Cell density was determined and VEGF secretion was normalized from pg/mL to pg/cell. Total volume of media was 2.5mL, total area of cell culture well was 1.9 cm^2. Table indicates ratio of VEGF release of HyA_CMNP, HyA_MNP, HyA_C, HyA_, CMNPs, MNPs, and C compared with BMSCs only.

4. Discussion

The objective of this study was to evaluate the effect of bare and hydrogel-loaded curcumin and curcumin-coated MNPs on BMSC activity, with emphasis on VEGF secretion. Curcumin coated magnetic iron oxide nanoparticles (CMNPs) were synthesized from a previously published co-precipitation method. Morphology, size, magnetic response, cytocompatibility, and effect on VEGF secretion was evaluated for CMNPs. The HyA loaded with CMNPs showed potential for proangiogenic bone tissue engineering applications.

4.1 Curcumin Coated Magnetic Nanoparticles

4.1.1 Characterization of Curcumin Coated Nanoparticles

The CMNPs had an average diameter of 17 nm which was 1 nm greater than MNPs. It is possible that the additional width was due to the curcumin coating, which would imply that the curcumin coating had a thickness of 0.5 nm. This small coating thickness can account for the fact that curcumin was not detected in TEM or XRD. However, the coating was detected by EDS, which showed much higher carbon presence in CMNP compared to MNP. XRD spectrum of stabilized CMNPs also confirmed magnetite structure. Magnetic iron oxide has a mixture of Fe_3O_4 and Fe_2O_3. Fe_3O_4 can oxidize to form Fe_2O_3 which is much less magnetic. The presence of curcumin likely protected the magnetic iron oxide from oxidation thereby preserving its magnetic properties. This is consistent with previous studies evaluating the ferromagnetic properties of CMNPs done by Bhandari R. et al, which also showed no significant difference in CMNP and MNP size, suggesting the synthetic process does not alter particle morphology [13]. The study also confirmed that curcumin

is difficult to distinguish through XRD analysis, however EDS analysis confirms the presence through a large atomic percentage of carbon.

CMNPs and MNPs were responsive to external magnetic force which confirmed their paramagnetic property. The paramagnetic property enabled the magnetic nanoparticles to align in the same direction as the external magnetic field in air and in water (Figure 4). In addition, once the external magnet was removed, the nanoparticles were no longer able to retain magnetization and became dispersed in water again, demonstrating prevention of nanoparticle agglomeration. This is important for maintaining nano-sized particles and allowing for nanoparticles to be cleared out quickly.

Absorbance measurements were utilized to evaluate curcumin release from CMNPs. The absorbance of rSBF exposed to CMNPs after 9 days exceeded that of the curcumin control, which would indicate more curcumin release than possible. However, there was also increase in absorbance of MNPs, which have no curcumin. When media was collected, a magnet was used to keep CMNPs and MNPs in their respective wells. However, if the magnetite oxidized, it would lose its magnetic property. It is likely that the increase in absorbance of MNPs came from oxidized nanoparticles. This is also likely the case for CMNPs because curcumin is water soluble and the coating may decrease over several days. This is supported by the increase in slope of absorbance change after day 5 for CMNPs. The curcumin control was completely solubilized, which is why its release spiked at day 1 and then stayed constant, as expected.

4.1.2 BMSC compatibility with CMNPs

After exposure to CMNPs, BMSCs exhibited healthy morphology. However, cell spreading appeared much greater in cells exposed to curcumin. This is consistent with previous studies that showed similar phenomena with vascular smooth muscle cells [19]. Spreading and elongation was less prevalent when BMSCs were exposed to 1000 μg/mL of CMNPs, MNPs, or curcumin. This may suggest that higher concentrations of curcumin may be toxic to cells but in the concentrations evaluated there was no significant decrease when compared to the BMSCs Only indicating that, CMNPs and MNPs are safe up to 1000 μg/mL. Post-culture pH showed variance from 8.7 to 8.9 for all samples. While some pH measurements may be mathematically significant, the difference was so small it is within error of the pH meter and is not physiologically relevant. Any pH change that may have been caused by the specific materials was compensated for by bicarbonate buffer present in DMEM.

4.2 Hyaluronic Acid Hydrogels with CMNPs

4.2.1 Hydrogel Swelling, Degradation

Presence of curcumin and iron oxide had great impact on the swelling behavior of these hydrogels. Samples with coated and non-coated MNPs resulted in greater swelling after 24 hours compared to HyA, indicating that iron oxide increases swelling. This may be due to increased hydrophilicity as iron oxide is polar. Additionally, oxide species are known to increase degradation of hyaluronic acid, which would lead to swelling and loss of shape[20, 21]. This is supported by the fact that HyA_MNP completely degraded within 9 days, in comparison to its counterpart with CMNP, where the curcumin coating protected

the hyaluronic acid from oxide release. Additionally, HyA_C showed less swelling overall which is most likely due to the hydrophobic nature of curcumin.

4.2.2 Magnetic Response of Hydrogels

HyA_CMNP was more responsive to magnetic stimulation compared to HyA_MNP. During incubation, it is likely that the MNPs within HyA_MNP oxidized, resulting in loss of magnetic response as shown in Figure 9. CMNPs protected MNPs from oxidation as curcumin acts as a protective coating stabilizing the molecule. Curcumin is also hydrophobic, which protect the particles against water. The curcumin coating protects again oxidation of the MNPs, resulting in hydrogels that are more magnetically responsive (13). Future studies can be done to quantify oxidation rates of nanoparticles by magnometry. A hysteresis curve can be analyzed for multiple samples at different time points of incubation in rSBF. Fe_3O_4 represented the magnetic form of iron oxide and therefore the hysteresis curve can determine oxidation rates based on changes in magnetism.

4.2.3 BMSC compatibility with CMNPs

After exposure to HyA_CMNP, HyA_MNP, HyA_C, HyA, CMNPs, MNPs, and C, BMSCs exhibited healthy morphology. Cells incubated in the presence of HyA_CMNP, HyA_C, CMNPs, and C showed elongated morphology due to the presence of curcumin which has been shown to allow for enhanced cell spreading [19]. Cell adhesion density was greater in the presence of hyaluronic acid, specifically in HyA_CMNP, HyA_MNP, HyA_C, and HyA groups compared to CMNPs, MNPs, C, and cells only control. Hyaluronic acid hydrogels have been shown to increase cell viability and enhance cell

function by providing a 3D structure for the cells. HyA gels provide cells with a microenvironment that is similar to 3D soft tissue, which allows them to remain viable and proliferate [1]. CMNPs have also been shown to increase cell viability and adhesion due to antioxidant properties of curcumin confirming that both HyA and CMNP enhanced viability of BMSCs [13]. This is supported by BMSCs culture with CMNPs having greater cell adhesion than other nanoparticle groups.

4.2.4 Post-Culture Media Analysis

To better understand the effects of hydrogel degradation on BMSCs, pH was measured. Hyaluronic acid degrades via abstraction of the hydrogen on the carbon adjacent to the carboxyl group in the n-glucuronic acid unit by hydroxyl radicals, which leads to glycosidic cleavage [16]. This causes more free hydrogens in solution causing a slight fluctuation in pH.

Ionic iron concentration was measured to determine if the hydrogels and nanoparticles released Fe^{2+}. However, only HyA_MNP had significantly lower Fe^{2+} concentration compared to Media. This indicated that the growth of cells resulted in decreased media Fe^{2+} from normal cell metabolism. In general, there is also no meaningful release of Fe^{2+} from the nanoparticles, whether bare or in hydrogels. The low levels of Fe^{2+} is due to the requirement of Fe^{2+} in developing cells. Cells, in the body, tend to acquire Fe^{2+} from plasma [24].

While HyA_CMNP and HyA showed statistically less Ca^{2+} than the media control the difference is less than 0.6 mM, which may not be physiologically relevant. It is also likely that cell metabolism had greater effect on Ca^{2+} concentration than the experimental

materials. This is supported by the fact that HyA_CMNP had the greatest cell density of all the samples.

Absorbance was utilized to measure curcumin released from hydrogels. As expected, HyA, CMNP, HyA_C, and C showed significantly higher absorbance compared to all other samples. However, HyA_CMNP and HyA_C had lower average absorbance than C, indicating that loading CMNPs and C into a hydrogel allowed for slow release of curcumin.

4.3 Effect of Hydrogels on VEGF Secretion

Cell density showed that the HyA_CMNP group had the higher cell viability and adhesion density on average compared to HyA_MNP, HyA_C, HyA, CMNPs, MNPs, C, and cells only groups. In addition, when compared to the BMSCs only control, HyA_CMNP, HyA_MNP, CMNPs, MNPs, and C groups have higher cell adhesion and viability. Deviations were too large to show statistical significance. A study with more duplicates may illuminate statistically significant increase in cell density when exposed to HyA_CMNP. It was hypothesized that is that curcumin, as well as the synergistic effect of hyaluronic acid hydrogels and magnetic nanoparticles, improved BMSC adhesion and enhance cell viability. Zhang et al. did a similar study and proposed that the combined effect of providing cells with a hydrogel to mimic extracellular matrix of soft tissue and the interaction of magnetic nanoparticles with BMSCs might be beneficial for cell adhesion. Cell adhesion is necessary for proper cellular function and tissue growth[13]. Each magnetic nanoparticle is a small source of a magnetic field, however when a gel is made with many nanoparticles the magnetic field effect is increased. The magnetic field

may affect ion channels and cause changes in cytoskeletal architecture. Fe_3O_4 nanoparticles have been shown to increase mesenchymal stem cell growth because off their ability to reduce intracellular H_2O_2 through intrinsic peroxidase-like activity. Previous studies also suggest that magnetic nanoparticles could accelerate cell cycle progression [22]. These effects can be further studied at different time points to determine long term cytocompatibility. Additionally, longer time points can be studied to determine differentiation potential of BMSCs in response to the gels.

Exposure to HyA_CMNP resulted in dynamic effects of VEGF secretion. Overall release of VEGF was greatest in HyA_CMNP but this was not true of secretion of VEGF/cell. This may be due to the fact that HyA_CMNP also resulted in highest cell density. It is possible that a feedback mechanism prevented the cells from releasing more VEGF. While curcumin alone did not increase adherent cell density, it did result in the highest VEGF secretion per cell. This is in agreement with previous studies which showed that BMSCs increase VEGF production. Previous studies have shown curcumin to increase VEGF secretion in adipose derived stem cells, which confirms that curcumin does have the potential to increase cytokine release [23].

5. Conclusions

The HyA_CMNP may prove as a promising method of localizing tissue regeneration oriented cell and drug delivery because the magnetic nanoparticles are responsive to an external magnetic field and the gel has been proven to maintain BMSCs viability and protein retention. We demonstrate that HyA_CMNP is beneficial to the activity of BMSCs by increasing cell density and overall VEGF production. Curcumin

prevents oxidation of iron oxide nanoparticles which in turn allows for avoiding oxidative toxicity when magnetic nanoparticles are used to enhance cell survivability and function. Curcumin also allows for hydrogels to maintain structural integrity for longer periods of time which can be useful for therapy development. Further cell studies in the presence of curcumin coated nanoparticles are needed to determine the combined effects of magnetic nanoparticles with a magnetic field on cell functions. Furthermore, in vivo testing needs to be done to determine the actual effects of the particles in real body conditions and to also display localization. In addition, 3D BMSC culture can be done by encapsulating cells into hydrogels and imaging using confocal microscopy to understand how cells will behave in vivo and studied as a localizable delivery vector for cells. Gels can be made to maintain structural integrity longer by using more crosslinker. Further evaluation of HyA_CMNP is recommended, particularly with endothelial cells, to fully elucidate its angiogenic effect.

6. Acknowledgements

The authors thank the support from the U.S. National Science Foundation (NSF award CBET 1512764), the Burroughs Wellcome Fund (1011235), the Hellman Faculty Fellowship (HL), and the University of California (UC) Regents Faculty Development Award (HL). The authors appreciate the Central Facility for Advanced Microscopy and Microanalysis (CFAMM) for the use of SEM FEI XL30 at the University of California at Riverside. The authors would also like to thank Anthony Del Torre for assistance with cell counts, Chaoxing Zhang for assistance with ICP-OES, Naiyin Zhang for guidance, and Shereen Aldaimalani for extensive proof reading.

7. References

1. Jha, A.K., et al., *Enhanced survival and engraftment of transplanted stem cells using growth factor sequestering hydrogels.* Biomaterials, 2015. **47**: p. 1-12.

2. Liu, H., et al., *In vivo liver regeneration potential of human induced pluripotent stem cells from diverse origins.* Sci Transl Med, 2011. **3**(82): p. 82ra39.

3. Matsuura, K., et al., *Transplantation of cardiac progenitor cells ameliorates cardiac dysfunction after myocardial infarction in mice.* J Clin Invest, 2009. **119**(8): p. 2204-17.

4. Min, J.Y., et al., *Significant improvement of heart function by cotransplantation of human mesenchymal stem cells and fetal cardiomyocytes in postinfarcted pigs.* Ann Thorac Surg, 2002. **74**(5): p. 1568-75.

5. Mizuno, Y., et al., *Generation of skeletal muscle stem/progenitor cells from murine induced pluripotent stem cells.* FASEB J, 2010. **24**(7): p. 2245-53.

6. Jha, A.K., et al., *Molecular weight and concentration of heparin in hyaluronic acid-based matrices modulates growth factor retention kinetics and stem cell fate.* Journal of Controlled Release, 2015. **209**: p. 308-316.

7. Langer, R. and J.P. Vacanti, *Tissue Engineering.* Science, 1993. **260**(5110): p. 920-926.

8. Liu, X. and P.X. Ma, *Polymeric scaffolds for bone tissue engineering.* Ann Biomed Eng, 2004. **32**(3): p. 477-86.

9. Ma, P.X., et al., *Engineering new bone tissue in vitro on highly porous poly(alpha-hydroxyl acids)/hydroxyapatite composite scaffolds.* J Biomed Mater Res, 2001. **54**(2): p. 284-93.

10. Vacanti, C.A. and J.P. Vacanti, *Bone and cartilage reconstruction with tissue engineering approaches.* Otolaryngol Clin North Am, 1994. **27**(1): p. 263-76.

11. Kaigler, D., et al., *Role of vascular endothelial growth factor in bone marrow stromal cell modulation of endothelial cells.* Tissue Engineering, 2003. **9**(1): p. 95-103.

12. Young, S., et al., *Microcomputed tomography characterization of neovascularization in bone tissue engineering applications.* Tissue Engineering Part B-Reviews, 2008. **14**(3): p. 295-306.

13. Bhandari, R., et al., *Single step synthesis, characterization and applications of curcumin functionalized iron oxide magnetic nanoparticles.* Materials Science & Engineering C-Materials for Biological Applications, 2016. **67**: p. 59-64.

14. Gupta, A.K. and M. Gupta, *Synthesis and surface engineering of iron oxide nanoparticles for biomedical applications.* Biomaterials, 2005. **26**(18): p. 3995-4021.

15. Kant, V., et al., *Curcumin-induced angiogenesis hastens wound healing in diabetic rats.* Journal of Surgical Research, 2015. **193**(2): p. 978-988.

16. Liu, J.F., et al., *Pretreatment of Adipose Derived Stem Cells with Curcumin Facilitates Myocardial Recovery via Antiapoptosis and Angiogenesis.* Stem Cells International, 2015.

17. Maheshwari, R.K., et al., *Multiple biological activities of curcumin: A short review.* Life Sciences, 2006. **78**(18): p. 2081-2087.

18. Tian, Q.M., et al., *Cytocompatibility of Magnesium Alloys with Human Urothelial Cells: A Comparison of Three Culture Methodologies.* Acs Biomaterials Science & Engineering, 2016. **2**(9): p. 1559-1571.

19. Grabowska, W., et al., *Curcumin induces senescence of primary human cells building the vasculature in a DNA damage and ATM-independent manner.* Age, 2015. **37**(1).

20. Yui, N., T. Okano, and Y. Sakurai, *Photo-responsive degradation of heterogeneous hydrogels comprising crosslinked hyaluronic acid and lipid microspheres for temporal drug delivery.* Journal of Controlled Release, 1993. **26**(2): p. 141-145.

21. Nobuhiko, Y., O. Teruo, and S. Yasuhisa, *Inflammation responsive degradation of crosslinked hyaluronic acid gels.* Journal of Controlled release, 1992. **22**(2): p. 105-116.

22. Huang, D.M., et al., *The promotion of human mesenchymal stem cell proliferation by superparamagnetic iron oxide nanoparticles.* Biomaterials, 2009. **30**(22): p. 3645-3651.

23. Cipriano, A.F., et al., *Investigation of magnesium-zinc-calcium alloys and bone marrow derived mesenchymal stem cell response in direct culture.* Acta Biomater, 2015. **12**: p. 298-321.

24. Wang, Jian, and Kostas Pantopoulos. "Regulation of cellular iron metabolism." *Biochemical Journal* 434.3 (2011): 365-381.

25. Zhang, Naiyin, et al. "Magnetic nanocomposite hydrogel for potential cartilage tissue engineering: synthesis, characterization, and cytocompatibility with bone marrow derived mesenchymal stem cells." (2015).